Materials Science and Engineering: C (2015). 49, 400-407.
DOI: http://dx.doi.org/10.1016/j.msec.2015.01.043

Feasibility Study of the Production of Biomedical Ti-6Al-4V Alloy by Powder Metallurgy

L. Bolzoni*, E.M. Ruiz-Navas, E. Gordo

Departamento de Ciencia e Ingeniería de Materiales e Ingeniería Química
Universidad Carlos III de Madrid, Avda. de la Universidad, 30, 28911 Leganés (Madrid), Spain
*e-mail: bolzoni.leandro@gmail.com

Abstract

Titanium and its alloys are characterized by an exceptional combination of properties like high strength, good corrosion resistance and biocompatibility which makes them suitable materials for biomedical prosthesis and devices. The wrought Ti-6Al-4V alloy is generally favored in comparison to other metallic biomaterials due to its relatively low elastic modulus and it has been long used to obtain products for biomedical applications. In this work an alternative route to fabricate biomedical implants made out of the Ti-6Al-4V alloy is investigated. Specifically, the feasibility of the conventional powder metallurgy route of cold uniaxial pressing and sintering is addressed by considering two types of powders (i.e. blended elemental and prealloyed). The characterization of physical properties, chemical analysis, mechanical behavior and microstructural analysis is carried out in-depth and the properties are correlated among them. On the base of the results found, the produced alloys are promising materials for biomedical applications as well as cheaper surgical devices and tools.

Keywords: titanium alloys, Ti-6Al-4V, powder metallurgy, tensile properties, dynamic Young modulus

1. Introduction

Titanium, a relatively new lightweight engineering material, is characterized by the highest specific strength (strength to density ratio), excellent corrosion resistance and outstanding biocompatibility [1]. Based on this, titanium should have a wide range of applications; nonetheless, this metal has always been used in high performance and high demanding industry, such as aerospace or medicine, where its combination of properties dominate over affordability issues [2]. This is mainly due to the production costs of this material, both extraction and processing costs, compared to competitive materials. The most widely used titanium alloys, the Ti-6Al-4V, is mainly employed to fabricate aerospace components as well as biomedical implants [3]. Titanium and titanium alloys for fixed and removable dental prostheses and devices are commonly obtained by casting processes such as centrifugal casting [4, 5] although some alternative techniques have been investigated to produce [6-10] or modify their surface [11, 12]. When casting is used, machining is generally employed to removed the brittle reaction layer (α-case) [13, 14] that forms from the interaction between molten titanium and the processing tools (i.e. oxide-based ceramic moulds and coating). Powder metallurgy (PM) techniques could offer the possibility to lower the final cost even if the starting material, a micrometric powder, is normally more expensive than an ingot combined with other important advantages in using PM method to fabricate titanium alloys. In particular, reduction of the fabrication costs by PM is primarily possible thanks to the more efficient material utilization (yield) and limited or unnecessary machining [15]. Furthermore, using PM techniques equivalent mechanical properties can be obtained and new composition unsuitable for ingot metallurgy can be produced. Finally, the requirements for the processing tools (sintering tray) are less stringent since the material does not reach the molten state during processing, such as in casting, and the formation of the α-case is limited or prevented. The purpose of this study is to determine whether the biomedical Ti-6Al-4V alloy can be produced by means of the conventional PM route of cold uniaxial press plus vacuum sinter.

Specifically, the variation of some physical, mechanical and microstructural features along with one of the most important parameter for PM processing, the sintering temperature, are considered. Moreover, the analyses carried out allow discovering whether there was some contamination during the processing of the materials and differentiate the influence of the powder production process, precisely, the prealloying and the master alloying approaches. The whole study was set to assess the feasibility of the production of cheaper structure structural biomedical, and in particular dental, prostheses, devices and tools.

2. Materials and Method

2.1 Ti-6Al-4V starting powders

The staring materials were a blended powder, labeled as Ti-6Al-4V-BE, and a prealloyed powder, identified as Ti-6Al-4V-PA. The description of the optimization of the purchased master alloy to produce the Ti-6Al-4V-BE alloy can be found in a previously published work [16]. As it can be seen in Figure 1 which shows SEM pictures of the starting powders, both powders are characterized by an irregular morphology which is dictated by their production method (i.e. HDH), a comminution process. The powders have similar particle size distribution (<90 μm) but the Ti-6Al-4V-PA powder is somewhat finer than the Ti-6Al-4V-BE powder. From the BSE micrograph of the Ti-6Al-4V-BE powder (Figure 1 c), the starting powders used to fabricate this alloy can be identified: elemental titanium, an Al:V master alloy and elemental aluminum. The particle size of the Al:V master alloy was reduced by high energy ball milling meanwhile mixed with the elemental aluminum powder [16]. Due to the intrinsic nature of the materials (i.e. ductile aluminum and brittle Al:V), the highly deformed aluminum powder particles tend to embed some of the Al:V particles. From Figure 1d, the Ti-6Al-4V-BE powder is characterized by an uniform distribution of the alloying elements. The contents of oxygen and nitrogen (ASTM: E1409) determined in the Ti-6Al-4V-BE and Ti-6Al-4V-PA powders are O = 0.43 wt.% and N = 0.012 wt.% and O = 0.42 wt.% and N =

0.010 wt.%, respectively. The total amount of oxygen dissolved in the starting powders is already higher than the value of the wrought Ti-6Al-4V (i.e. 0.20 wt%) whilst the content of nitrogen is lower than the limit specified for the ELI (extra-low interstitials) grade of the Ti-6Al-4V alloy whose maximum is 0.03 wt.% [17].

2.2 Consolidation of the Ti-6Al-4V materials

The loose powders were poured inside the cavity of a floating die whose die-walls were lubricated with zinc stearate and consolidated with a uniaxial press. It is important to remark that no lubricant was added on purpose to the Ti-6Al-4V powders to limit as much as possible to contamination of the starting powders. The geometry of the specimens chosen for this study is the one known as "dogbone" (ASTM: B925) to be tested to measure tensile properties. For the sintering of the green samples an electrical resistance tubular furnace was used and sintering was carried out under high vacuum (10^{-5} mbar). Based on previous studies [18, 19], the sintering temperature window was set to laid between 1250ºC and 1350ºC while the dwell time was fixed at 2 hours. It is worth mentioning that a minimum of three samples were considered for each processing condition.

2.3 Characterization of the sintered Ti-6Al-4V materials

The variation of the dimensions induced by the sintering step was considered and for that the dimensions of green and sintered specimens were measured. The relative density values (ρ_r) was calculated as: (ρ_s/ρ_{nom} *100) where ρ_s is the density of the sintered samples and the (ρ_{nom}) is the nominal density of the Ti-6Al-4V alloy (4.43 g/cm^3) [17]. As for the powders, the calibrated LECO TC500 was used to measure the contents of interstitial elements of the sintered materials. The preparation of the samples for their microstructural analysis included: cut, grinding with SiC papers of different granulometry, polishing with silica gel and etching with Kroll' reactant. Vickers hardness (HV30) measurements were performed in a Wilson

Wolpert DIGI-TESTOR 930 Universal Hardness tester. Tensile tests, done on the base of the ASTM: E8 standard, were performed on a MicroTest universal machine. The crosshead speed was set to 1 mm/min. Yield strength values were calculated by means of the off-set method. The fractographic study of the tensile samples was done using a Philips XL-30 SEM. For tensile specimens, the dynamic elastic modulus (E) determined by the speed of sound (ν) and the relative density was considered to avoid possible artifacts intrinsic of the stress-strain curves and it calculated using equation 1:

$$v = \sqrt{E/\rho_r} \qquad \text{(Eq. 1)}$$

An ultrasonic transducer (Grindosonic) having a frequency range in between 20 Hz and 100 KHz and an accuracy better than 0.005% was employed for determining the speed of sound. Throughout the whole work, the properties (i.e. microstructure, hardness, yield strength, ultimate tensile strength, strain and Young modulus) of the sintered Ti-6Al-4V materials are compared to those of the wrought Ti-6Al-4V in the typical mill annealed state (750ºC during 4 hours, furnace cooled) whose microstructure is composed of globular particles of β in a matrix of α [17].

3. Results

3.1 Physical properties of the sintered Ti-6Al-4V materials

The green density of the cold uniaxially pressed tensile test samples with “dogbone” geometry is 86.56% ± 0.38% for Ti-6Al-4V-BE and 81.98% ± 0.49% for Ti-6Al-4V-PA, respectively. The variation of the dimensions of the samples and of the relative density are presented in Figure 2.

Analyzing the data of the shrinkage underwent form the green samples during the sintering step (Figure 2 a), it can be seen that the shrinkage increases linearly with the increment of the sintering temperature from 1250ºC to 1350ºC where this increment is much more noticeable for the Ti-6Al-4V-BE alloy than for the Ti-6Al-4V-PA alloy. More in detail, in the case of the

Ti-6Al-4V-BE alloy the increment is somewhat less pronounced when raising the temperature from 1250ºC to 1300ºC (i.e. 0.22%) than from 1300ºC to 1350ºC (i.e. 0.27%) whilst the increment of the shrinkage with the processing temperature is constant (i.e. 0.04%) for the Ti-6Al-4V-PA alloy. For the Ti-6Al-4V-BE alloy part of thermal energy supplied to the system is spent for the diffusion of the alloying elements towards the titanium matrix, which is not the case for the Ti-6Al-4V-PA alloy where the total composition is already fully homogeneous. This aspect is responsible for the lower absolute shrinkage values that characterized the Ti-6Al-4V-BE alloy (about 4%) with respect to the Ti-6Al-4V-PA alloy (greater than 6%). As it can be seen in Figure 2b, generally, the relative density of the Ti-6Al-4V-BE and Ti-6Al-4V-PA alloys slightly increases with the sintering temperature. Specifically, the increment that the Ti-6Al-4V-BE samples experience during sintering is greater when increasing the processing temperature from 1250ºC to 1300ºC rather than from 1300ºC to 1350ºC where, actually, this last increment is less than half of the previous one. Conversely, in the case of the Ti-6Al-4V-PA alloy the increment in terms of relative density is quite homogeneous with the processing temperature. Because of these two relative trends the difference between the final relative density values of the Ti-6Al-4V-BE and Ti-6Al-4V-PA alloys becomes smaller but still the final relative density of the Ti-6Al-4V-PA alloy is, at least, 1% higher than that of the Ti-6Al-4V-BE alloy, which starts from a higher green density but undergoes lower shrinkage.

3.2 Chemical analysis of the sintered Ti-6Al-4V materials

The results of the chemical analysis done on sintered samples are presented in Table 1. From the data of the chemical analysis carried out on the sintered Ti-6Al-4V-BE and Ti-6Al-4V-PA alloys to determine the amount of interstitial elements dissolved (Table 1), it can be seen that the oxygen content increases with the increment of the processing temperature with the only exception of the Ti-6Al-4V-BE samples sintered at 1350ºC which are characterized

by the same content of oxygen of that of the specimens processed at 1300ºC. Conversely, in the case of nitrogen content there is not a clear trend with the increment of the processing temperature for either of the alloys considered. From the data of Table 1, it can also be noticed that, although of the employment of high vacuum, there is both oxygen and nitrogen pick-up with respect to the amount of these interstitials present in the starting powder regardless of the processing conditions used to sinter the green samples. On the one hand, the oxygen pick-up for the Ti-6Al-4V-BE alloy is quite limited (i.e. maximum 0.03 wt.%) whilst it is greater, between 0.05 wt.% and 0.14 wt.%, for the Ti-6Al-4V-PA alloy. On the other hand, the amount of nitrogen pick-up seems to be rather constant, because the final values lay between 0.019 wt% and 0.025 wt.%., and, thus, better limited by the sintering under high vacuum. The total amount of interstitial elements, but in this particular case especially oxygen because it is higher than that of the wrought alloy, will influence the mechanical behavior of the sintered Ti-6Al-4V-BE and Ti-6Al-4V-PA alloys. This is because the interstitials harden, strengthen and diminish the ductility of titanium and its alloys [20-22].

3.3 Microstructural analysis of the sintered Ti-6Al-4V materials

A microstructural analysis was carried out to study the development of the microstructure and the evolution of the porosity and the representative micrographs of both materials are displayed in Figure 3.

The microstructure of the Ti-6Al-4V-BE and Ti-6Al-4V-PA alloys sintered at 1250ºC (Figure 3 a and b) is composed of α grains and α+β lamellae of different orientation that remained after the growth of the α phase during cooling. Another feature of the microstructure of the sintered Ti-6Al-4V-BE and Ti-6Al-4V-PA alloys is the residual porosity that can be clearly be identified in their microstructures. On the one side, a great percentage of the residual porosity of the Ti-6Al-4V-BE alloy is still interconnected and irregular in shape indicating that the pores coalescence and coarsening did not take place completely yet even if spherical

pores are present. On the other hand, the residual porosity of the Ti-6Al-4V-PA alloy is practically spherical with very few coarse pores of irregular shape. An increment of the sintering temperature to 1300ºC or 1350ºC does not change the nature of the microconstituents (i.e. α grains and α+β lamellae) but it does induce their coarsening, which is especially notable in the components sintered at 1350ºC. Therefore, the microstructure of the Ti-6Al-4V-BE alloy is still coarser than that of the Ti-6Al-4V-PA alloy though the difference is not that marked as in the case of the samples processed at 1250ºC. Concerning the residual porosity, the increment of the sintering temperature leads to its volumetric percentage reduction but the mean size seems to be increased due to the fact that the pores tend to coalesce. In the case of the Ti-6Al-4V-BE alloy the residual porosity of the specimens processed at 1350ºC is mainly spherical, even if some irregular pores are still present, which it is not the case for the material sintered at 1300ºC.

Figure 4 shows the BSE micrographs of the Ti-6Al-4V-BE and Ti-6Al-4V-PA alloys where it can be seen that with the sintering parameters employed the complete diffusion and homogenization of the alloying elements is obtained.

The total amount of residual porosity, which can be clearly seen in the BSE images reported in Figure 4, decreases with the increment of the sintering temperature. The great majority of the pores are spherical in shape and located at the boundaries between adjacent α grains divided by the lamellae. The size distribution of the pore ranges between 20 μm to 50 μm with some few pores of bigger size (< 100 μm).

The results of the EDS analysis carried out to further confirm the homogeneous distribution of the alloying elements, which is paramount to guarantee reliable and consistent properties, are reported in Table 2.

3.4 Mechanical properties of the sintered Ti-6Al-4V materials

The results of hardness measurements for Ti-6Al-4V-BE and Ti-6Al-4V-PA alloys are shown in Figure 5.

From the data of the Vickers Hardness measurements performed into the cross-section of the sintered specimens (Figure 5), the hardness follows the same trend of the relative density and, therefore, it increases continuously with the increment of the sintering temperature. By a closer look to the absolute values, it can be noticed that the increment in terms of hardness that takes place between 1250ºC and 1300ºC is slightly greater than that between 1300ºC and 1350ºC. This fact is in agreement with the densification and the relative density (Figure 2 b) data and it is mainly a consequence of the phenomena that govern the sintering step.

The typical tensile stress-strain behavior found for Ti-6Al-4V-BE and Ti-6Al-4V-PA materials sintered in the range 1250-1350ºC is displayed in Figure 6.

As it can be seen in Figure 6, the typical tensile stress-strain curves for the Ti-6Al-4V processed by pressing and sintering are composed by an elastic part, up to approximately 800 MPa, and then some plastic deformation, which is around 3%. This plastic deformation gets lower with the sintering temperature. From the curves it can also be noticed that, independently of the sintering temperature, all the materials show similar shape indicating similar behavior and Young modulus.

The variation of the yield stress, ultimate tensile strength (UTS) and strain at fracture (ε) with the sintering temperature in comparison to the value of the wrought alloy is shown in Figure 7.

Analyzing the data shown in Figure 7, it can be seen that the yield stress slightly increases with the processing temperature and, in most of the cases, the values obtained are higher than the one specified for the wrought Ti-6Al-4V alloy. With respect to the UTS of the Ti-6Al-4V-BE alloy decreases from 900 MPa down to 810 MPa with the increasing of the sintering temperature whereas that of the Ti-6Al-4V-PA alloy stays practically constant. Concerning

the strain at fracture data (Figure 7), it can be seen that the ductility of both Ti-6Al-4V-BE and Ti-6Al-4V-PA alloys decreases with the temperature.

The fractographic analysis of the tensile test specimens by SEM was carried out and the results are presented in Figure 8.

From the analysis of the fracture surfaces (Figure 8), it can be seen that the materials present ductile fracture due to microvoids coalescence where the size of the dimples found in the Ti-6Al-4V-BE alloy seem to be larger than Ti-6Al-4V-PA. This pore-assisted fracture is the typical behavior of the Ti-6Al-4V titanium alloy obtained by the conventional PM route and it is similar to those formed on ingot metallurgy processed materials [23].

The results of the dynamic Young modulus carried out on Ti-6Al-4V-BE and Ti-6Al-4V-PA alloys sintered samples are reported in Table 3 where it can be seen that the measured values are very similar between them regardless of the sintering temperature which is in agreement with the results of the stress-strain curves (Figure 6).

4. Discussion

From the characterization of the starting powders and of the behavior of the Ti-6Al-4V-BE and Ti-6Al-4V-PA alloys, it can be stated that the irregular morphology of the Ti-6Al-4V powders makes them ideal and suitable materials to be processed by the conventional route of cold uniaxial pressing and sintering. This is because during cold pressing the asperities of the irregular powder particles deform and form the interparticles locking which constitute the green strength of the green components. This guarantees the handling of the parts without breakage or delamination which is paramount for maintaining the original shape of biomedical devices. Moreover, the difference in maximum particle size plays a role during the consolidation and the densification of the Ti-6Al-4V components because the smaller the particle size the greater the specific surface area where the reduction of the total surface area is one of the driving force of the sintering of particulate materials. More in detail, Ti-6Al-4V-

PA alloy has slightly lower green density but this is due to the fact that it has already the alloying elements dissolved inside the titanium matrix in each single powder particle. This aspect makes them harder and less deformable and, therefore, more difficult to shape by cold uniaxial pressing. Nevertheless, the Ti-6Al-4V-PA alloy is characterized by a higher contraction during sintering (i.e. shrinkage) and undergoes a much higher densification (somewhat lower than 80%) with respect to the Ti-6Al-4V-BE alloy (50-60%). This is due to the fact that none of the thermodynamic energy supplied to the system is invested in the diffusion of the alloying elements towards the titanium matrix and on the homogenization of the alloying elements throughout the whole microstructure. Because of these aspects, the Ti-6Al-4V-BE alloy reaches final lower relative density values, of at least 1% (Figure 2 b), where the difference in terms of relative density is more marked at lower sintering temperatures. Furthermore, the densification of the Ti-6Al-4V-PA alloy is also favored by the slightly lower powder particle size or, in turns, its bigger specific surface area. The sintering of the green Ti-6Al-4V-BE and Ti-6Al-4V-PA alloys components has two other main effects: interstitial pick-up and grain growth. Concerning the chemical analysis, oxygen and nitrogen pick-up are due to the handling of the powder, the air trapped into the green samples and to the oxygen and nitrogen atoms adsorbed on the surface of the powder particles which diffuse into the material during the sintering step. Nevertheless, the final amount of interstitials is also affected by the fact that sintering is carried out by batched and there could be slight variation in the atmosphere present inside the sintering furnace. In comparison to the typical values of the wrought Ti-6Al-4V alloy, the amount of oxygen dissolved by the Ti-6Al-4V-BE and Ti-6Al-4V-PA alloys is higher, as it was already the case for the starting powders, whereas the final nitrogen contents shown in Table 1 are still lower than the limit of the ELI grade. Regarding the microstructural analysis, the microstructure of the Ti-6Al-4V-BE and Ti-6Al-4V-PA alloys is the typical of the wrought Ti-6Al-4V alloy slow cooled from a processing temperature above the β transus (i.e. 996ºC), although finer with respect to wrought alloys,

and it is composed by α grains which started to grow from the beta grain and α+β lamellae. Moreover, by the comparison of the microstructure of the Ti-6Al-4V-BE and Ti-6Al-4V-PA alloys, it can be noticed that the microstructural features of the Ti-6Al-4V-BE alloy are slightly coarser than those of the Ti-6Al-4V-PA due to the fact that the Ti-6Al-4V-BE has slightly bigger starting particle size distribution. Another microstructural feature of the sintered Ti-6Al-4V-BE and Ti-6Al-4V-PA alloys is the presence of the residual porosity where this is smaller in size and lower in volumetric percentage for the Ti-6Al-4V-PA alloy in agreement with the relative density data shown in Figure 2 b). The increment of the sintering temperature leads to a coarsening of the microstructural features (i.e. grain growth and pores coalescence). On the base of the characterization and of the result just described, the Ti-6Al-4V-BE and Ti-6Al-4V-PA alloys have similar or higher hardness and comparable mechanical behavior (i.e. comparable ultimate tensile strength, the same microvoids coalescence ductile fracture mode and similar Young modulus) but lower ductility with respect to the wrought Ti-6Al-4V alloy. In particular, the hardness of the Ti-6Al-4V-BE and Ti-6Al-4V-PA alloys increases with the processing temperature where this increment is mainly due to the reduction of the volumetric amount of residual porosity present in the microstructure but is also favored by the oxygen and nitrogen pick-up that the component experience during sintering. By the comparison of the absolute hardness values of the two alloys studied, it can be seen that Ti-6Al-4V-PA samples always reach higher hardness of approximately 20 HV30 with respect to the Ti-6Al-4V-BE specimens. This is, once again, due to the combination of higher relative density (i.e. lower residual porosity) and higher oxygen content (Table 1) that characterizes the Ti-6Al-4V-PA sintered components. From the graph shown in Figure 5, it can also be seen that the sintered Ti-6Al-4V-BE and Ti-6Al-4V-PA alloys, generally, have comparable hardness to the wrought Ti-6Al-4V alloy with the exception of the samples made out of the Ti-6Al-4V-BE alloy sintered at 1250ºC. The fact that the sintered Ti-6Al-4V-BE and Ti-6Al-4V-PA reach similar hardness even though of the

presence of approximately 4-5% of residual porosity is due to the greater amount of oxygen dissolved into these materials. Actually, Ti-6Al-4V-PA alloy, which undergoes a higher oxygen pick-up during sintering, is characterized by an even higher Vickers hardness in comparison to the wrought Ti-6Al-4V alloy in the annealed state whose hardness is 320 HV [17]. The yield stress of both Ti-6Al-4V-BE and Ti-6Al-4V-PA alloys increases because of the reduction of the residual porosity and the strengthening mechanism of the oxygen present in the interstitial sites of the titanium lattice. The specific level of oxygen of each sintering condition also helps to explain the differences between the two materials (i.e. Ti-6Al-4V-PA alloy has higher oxygen and, thus, higher yield strength) and the difference with respect to the value of the Ti-6Al-4V wrought alloy (Figure 7). Specifically, Ti-6Al-4V-BE and Ti-6Al-4V-PA alloys have higher yield strength than the wrought alloy, although of the presence of the residual porosity, because of their higher oxygen content. The ultimate tensile strength of the Ti-6Al-4V-BE alloy decreases with the sintering temperature and that of the Ti-6Al-4V-PA alloy remains constant and this different behavior is due to the combination of the lower relative density, lower oxygen content and coarser microstructure of the Ti-6Al-4V-BE and Ti-6Al-4V-PA alloys. Actually, it can be noticed that the difference becomes bigger with the increment of the sintering temperature whose effects are: reduce the difference in terms of relative density and size of the microstructural features but significantly enhance the difference in terms of oxygen content between the Ti-6Al-4V-BE and Ti-6Al-4V-PA alloys. By analyzing the UTS data shown in Figure 7, it can also be noticed that, apart from the Ti-6Al-4V-BE alloy sintered at 1350ºC, the UTS values obtained are similar to that of the wrought alloy (i.e. 900 MPa) despite the fact that the Ti-6Al-4V-BE and Ti-6Al-4V-PA alloys are characterized by the presence of the residual porosity as microconstituent (Figure 3). This behavior is justified by the fact that the Ti-6Al-4V-BE and Ti-6Al-4V-PA alloys have higher oxygen content and finer microstructural features in comparison to the wrought Ti-6Al-4V alloy in the annealed state. For both the Ti-6Al-4V-BE and Ti-6Al-4V-PA alloys the strain at

fracture decreases with the increment of the sintering temperature principally due to the interstitial elements pick-up. It is worth mentioning that the greatest drop in strain for the Ti-6Al-4V-BE alloy take place from 1250ºC to 1300ºC which is exactly when the amount of interstitial elements increases the most. In the case of the Ti-6Al-4V-PA alloy, the important drop in ductility occurs when increasing the sintering temperature from 1300C to 1350ºC which is, once again, when the material experience the greatest interstitials pick-up and pores coarsening. By the comparison of the strain at fracture data of the two alloys, it can be seen that the Ti-6Al-4V-PA alloy performs somewhat better than the Ti-6Al-4V-BE alloy despite of the grater oxygen content which is mainly due to the lower relative density or volumetric percentage of residual porosity of the Ti-6Al-4V-BE alloy where the size and shape of the pores play a paramount role. Whit respect to the wrought alloy (Figure 7), the ductility of both Ti-6Al-4V-BE and Ti-6Al-4V-PA alloys is lower due to the greater amount of interstitial elements and the residual porosity that characterize them. If needed, the final amount of residual porosity of the Ti-6Al-4V-BE and Ti-6Al-4V-PA alloys could be reduced or even eliminated by means of a post-processing of the materials by using a hot isostatic pressing cycle. For that the samples would need to be encapsulated in an inert container and degasified prior to proceed with their processing at a temperature below the beta transus of the alloy simultaneously applying isostatic pressure by means of an inert gas (i.e. argon). The reduction or sealing of the residual porosity is expected to improve the mechanical performances, especially under dynamic and cyclic loads (i.e. fatigue). Finally, both Ti-6Al-4V-BE and Ti-6Al-4V-PA alloys have similar elastic modulus to the wrought material and it does not vary significantly with the sintering temperature. This is thought to be due to the fact that the sintered alloy are characterized exclusively by closed porosity because their relative density is greater than 94%. Below this critical value the sintered materials present both open and closed porosity of relative density [15, 24] and, consequently, physical and mechanical properties are much more affected by the presence of the residual porosity. Specifically, the properties are

expected to have steeper decreasing linear correlation with the decrement of the relative density for values lower than 94% [25]. The variation of the mechanical properties reported in this work with the sintering temperature are consistent with the results found when assessing the sinterability of the Ti-6Al-4V-BE and Ti-6Al-4V-PA alloys over a wider range of processing temperatures (i.e. 900-1400ºC) [18, 19] or the influence of the sintering time [26]. It is worth mentioning in previous studies, in some cases, a lower compacting pressure was used. The lower the shaping pressure leads to lower green densities and, eventually a stronger effect of the residual porosity in the final behavior of the sintered alloys. In particular, in that part of this systematic study to assess different properties of titanium powder metallurgy materials processed under different combination of compacting and sintering parameters it was found that the mechanical properties increase linearly with the increment of the sintering temperature. Nonetheless, the mechanical performances (transverse rupture strength and strain) decrease starting approximately from the sintering temperature of 1300ºC. This is due to the fact that for the Ti-6Al-4V-BE and Ti-6Al-4V-PA alloys a critical amount of interstitials (especially oxygen) is reached with such processing condition. The tensile properties of the Ti-6Al-4V-BE and Ti-6Al-4V-PA alloys show similar behavior as discussed on the base of the results reported in Figure 7.

5. Conclusions

This feasibility study of the production of the biomedical Ti-6Al-4V alloy by powder metallurgy demonstrated that, actually, titanium alloys processed by means of the conventional powder metallurgy route of cold uniaxial pressing and (vacuum) sintering show similar mechanical behavior to that of the wrought alloy. The main advantage of the employment of powder metallurgy for the production of biomedical devices is the reduction of the final production cost and the possibility to consolidate components to their near-net shape. Irregular powders are suitable for the pressing and sintering route where the increment

of the sintering temperature leads to higher shrinkage and densification as well as relative density level regardless of the nature of the powder. A great range and combination of mechanical properties can be achieved by changing the processing temperature to adjust them for specific products. Moreover, the employment of different type of powders (namely, prealloyed or blending elemental) is another aspect which permits to wide the spectrum of properties achievable and required for different applications.

Acknowledgements

The authors want to acknowledge the financial support from Regional Government of Madrid through the ESTRUMAT (S2009/MAT-1585) project and from the Spanish Ministry of Science through the R&D Projects MAT2009-14547-C02-02 and MAT2009-14448-C02-02.

References

[1] C. Leyens, M. Peters, Titanium and Titanium Alloys. Fundamentals and Applications, Wiley-VCH, Köln, Germany, 2003.

[2] K. Roncone, O. Yu, C. Boland, R. Boyer, M. Mohanty, N. Murray, A. Sherman, JOM, 57 (2005) 11-13.

[3] D.M. Brunette, P. Tengvall, M. Textor, P. Thomsen, Titanium in medicine: Materials Science, Surface Science, Engineering, Biological Responses and Medical Applications, Springer, New York, USA, 2001.

[4] K. Watanabe, O. Miyakawa, Y. Takada, O. Okuno, T. Okabe, Biomaterials, 24 (2003) 1737–1743.

[5] P.C. Garcia Oliveira, G. Luis Adabo, R. Faria Ribeiro, S. Soares Rocha, Dental Materials, 22 (2006) 1098–1102.

[6] T. Traini, C. Mangano, R.L. Sammons, F. Mangano, A. Macchi, A. Piattelli, Dental Materials, 24 (2008) 1525–1533.

[7] V. Srimaneepong, T. Yoneyama, E. Kobayashi, H. Doi, T. Hanawa, Dental Materials, 24 (2008) 839–845.

[8] E. Marin, M. Pressacco, S. Fusi, A. Lanzutti, S. Turchet, L. Fedrizzi, Materials Science and Engineering: C, 33 (2013) 2648–2656.

[9] Z. Lin, L. Wang, X. Xue, W. Lu, J. Qin, D. Zhang, Materials Science and Engineering: C, 33 (2013) 4551–4561.

[10] G. Serra, L. Morais, C.N. Elias, I.P. Semenova, R. Valiev, G. Salimgareeva, M. Pithon, R. Lacerda, Materials Science and Engineering: C, 33 (2013) 4197–4202.

[11] F.J. Gil, J.A. Planell, J. Padros, C. Aparicio, Dental Materials, 23 (2007) 486–491.

[12] A. Poulon-Quintin, I. Watanabe, E. Watanabe, C. Bertrand, Dental Materials, 28 (2012) 945–951.

[13] S.-Y. Sung, Y.-J. Kim, Materials Science and Engineering: A, 405 (2005) 173-177.

[14] C. Ohkubo, T. Hosoi, J.P. Ford, I. Watanabe, Dental Materials, 22 (2006) 268–274.

[15] R.M. German, Powder Metallurgy Science, 2nd Edition ed., MPIF - Metal Powder Industries Federation, Princeton, USA, 1994.

[16] L. Bolzoni, P.G. Esteban, E.M. Ruiz-Navas, E. Gordo, Powder Metallurgy, 54 (2011) 543-550.

[17] R. Boyer, G. Welsch, E.W. Collings, in: A. International (Ed.), Ohio, USA, 1998.

[18] L. Bolzoni, P.G. Esteban, E.M. Ruiz-Navas, E. Gordo, Journal of the Mechanical Behavior of Biomedical Materials, 15 (2012) 33-45.

[19] L. Bolzoni, P.G. Esteban, E.M. Ruiz-Navas, E. Gordo, Journal of the Mechanical Behavior of Biomedical Materials, 14 (2012) 29-38.

[20] R.I. Jaffee, I.E. Campbell, Transactions of the American Institute of Mining and Metallurgical Engineers, 185 (1949) 646-654.

[21] R.I. Jaffee, H.R. Ogden, D.J. Maykuth, Transactions of the American Institute of Mining and Metallurgical Engineers, 188 (1950) 1261-1266.

[22] W.L. Finlay, J.A. Snyder, Journal of Metals 188 (1950) 277-286.

[23] J.E. Smugeresky, D.B. Dawson, Powder Technology, 30 (1981) 87-94.

[24] G. Friedman, R. Regn, Metal Powders Report, 39 (1984) 273-281.

[25] C. Vincent, J.F. Silvain, J.M. Heintz, N. Chandra, Journal of Physics and Chemistry of Solids, 73 (2012) 499-504.

[26] L. Bolzoni, E.M. Ruiz-Navas, E. Gordo, Materials and Design, 52 (2013) 888-895.

Figure 1. SEM pictures showing the morphology (a and b) and the composition (c and d) of the starting powders, respectively: a) Ti-6Al-4V-BE and b) Ti-6Al-4V-PA alloys.

Figure 2. Variation of the thickness (a) and of the relative density (b) as a function of the sintering temperature for the Ti-6Al-4V-BE and Ti-6Al-4V-PA alloys.

Figure 3. Optical micrographs of the Ti-6Al-4V-BE and Ti-6Al-4V-PA alloys sintered at 1250ºC: a) Ti-6Al-4V-BE and b) Ti-6Al-4V-PA, at 1300ºC: c) Ti-6Al-4V-BE and d) Ti-6Al-4V-PA and at 1350ºC: e) Ti-6Al-4V-BE and f) Ti-6Al-4V-PA.

Figure 4. SEM (BSE) micrographs of the Ti-6Al-4V-BE and Ti-6Al-4V-PA alloys sintered at 1250ºC: a) Ti-6Al-4V-BE and b) Ti-6Al-4V-PA, at 1300ºC: c) Ti-6Al-4V-BE and d) Ti-6Al-4V-PA and at 1350ºC: e) Ti-6Al-4V-BE and f) Ti-6Al-4V-PA.

Figure 5. Variation of the hardness as a function of the sintering temperature for the Ti-6Al-4V-BE and Ti-6Al-4V-PA alloys.

Figure 6. Representative stress-strain behaviour of sintered Ti-6Al-4V alloys: a) Ti-6Al-4V-BE and b) Ti-6Al-4V-PA.

Figure 7. Variation of the tensile properties as a function of the sintering temperature for the Ti-6Al-4V-BE and Ti-6Al-4V-PA alloys: left) ultimate tensile strength - UTS and right) strain at fracture (ε).

Figure 8. Fracture surface of the Ti-6Al-4V-BE and Ti-6Al-4V-PA alloys sintered at 1250ºC: a) Ti-6Al-4V-BE and b) Ti-6Al-4V-PA.

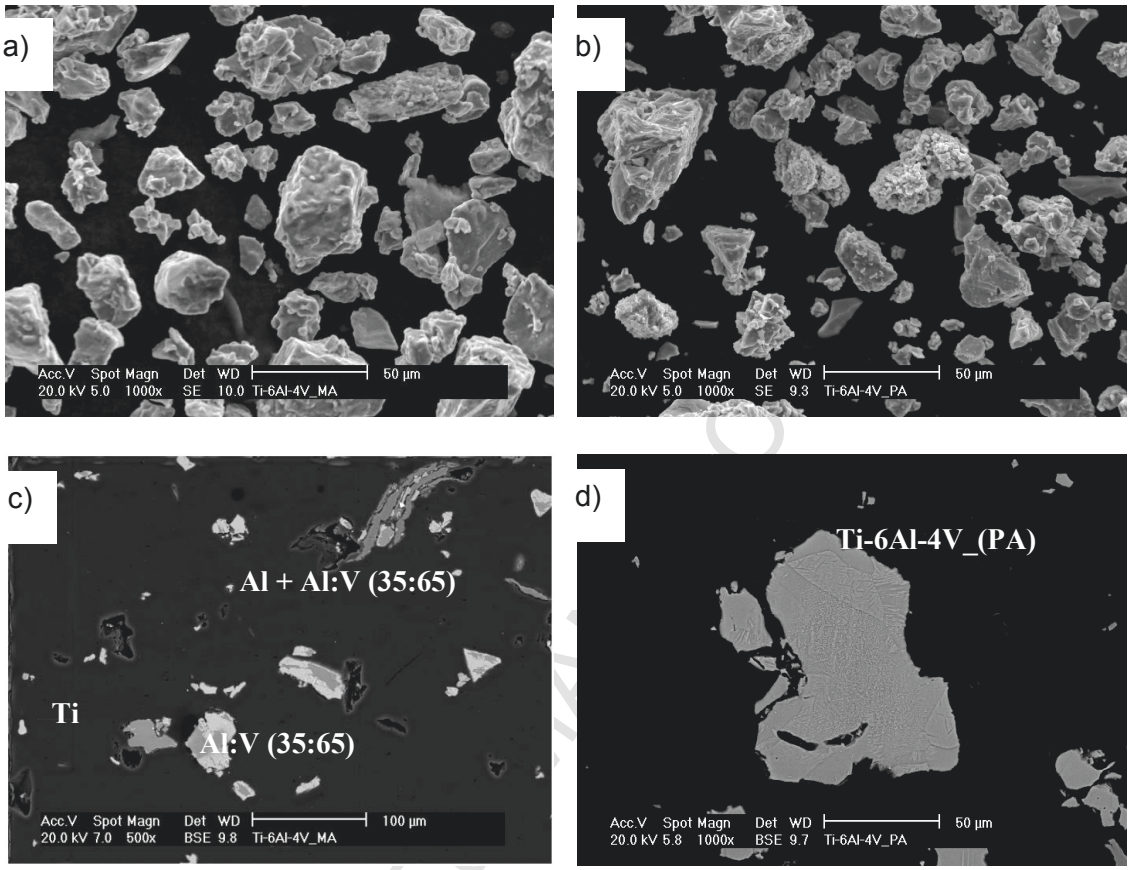

Fig. 1

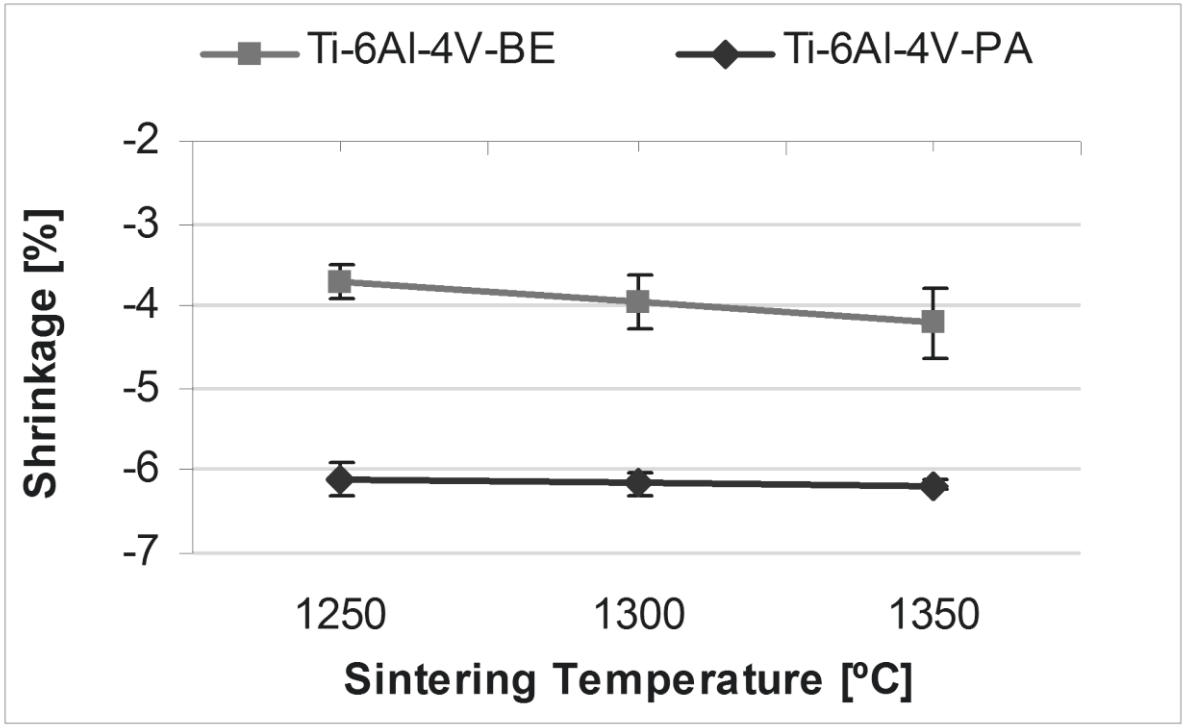

Fig. 2a

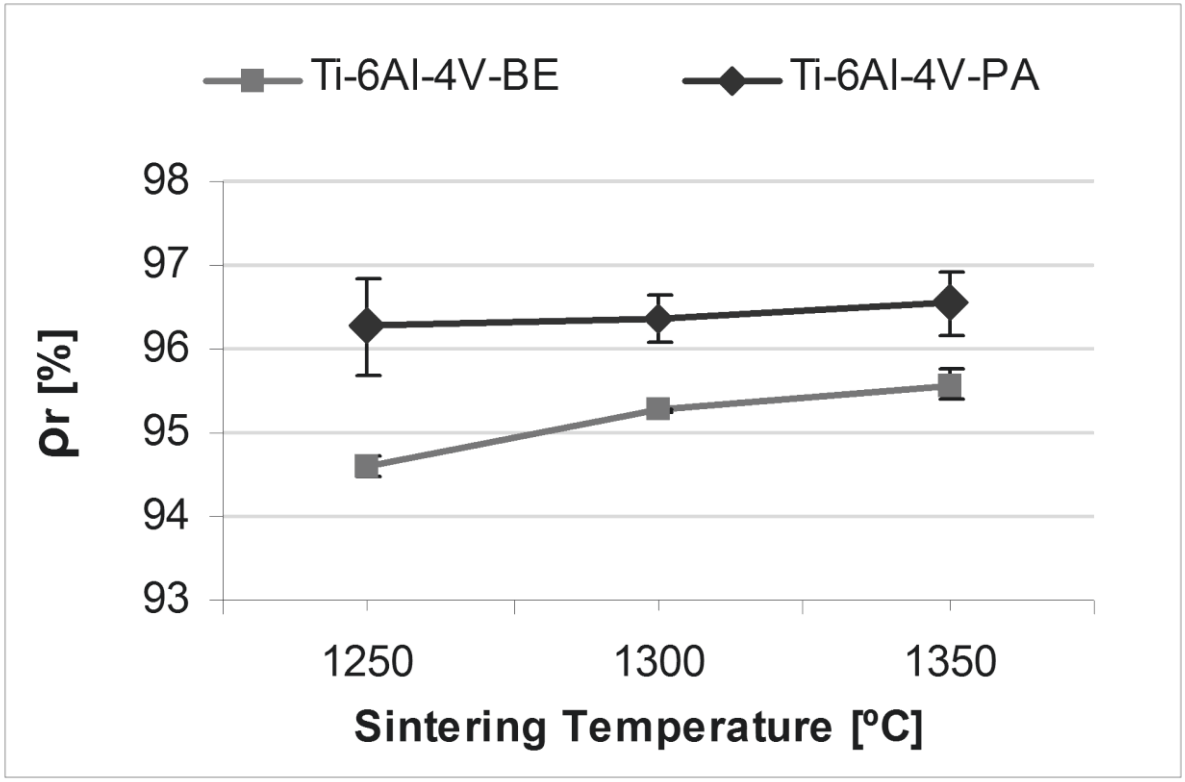

Fig. 2b

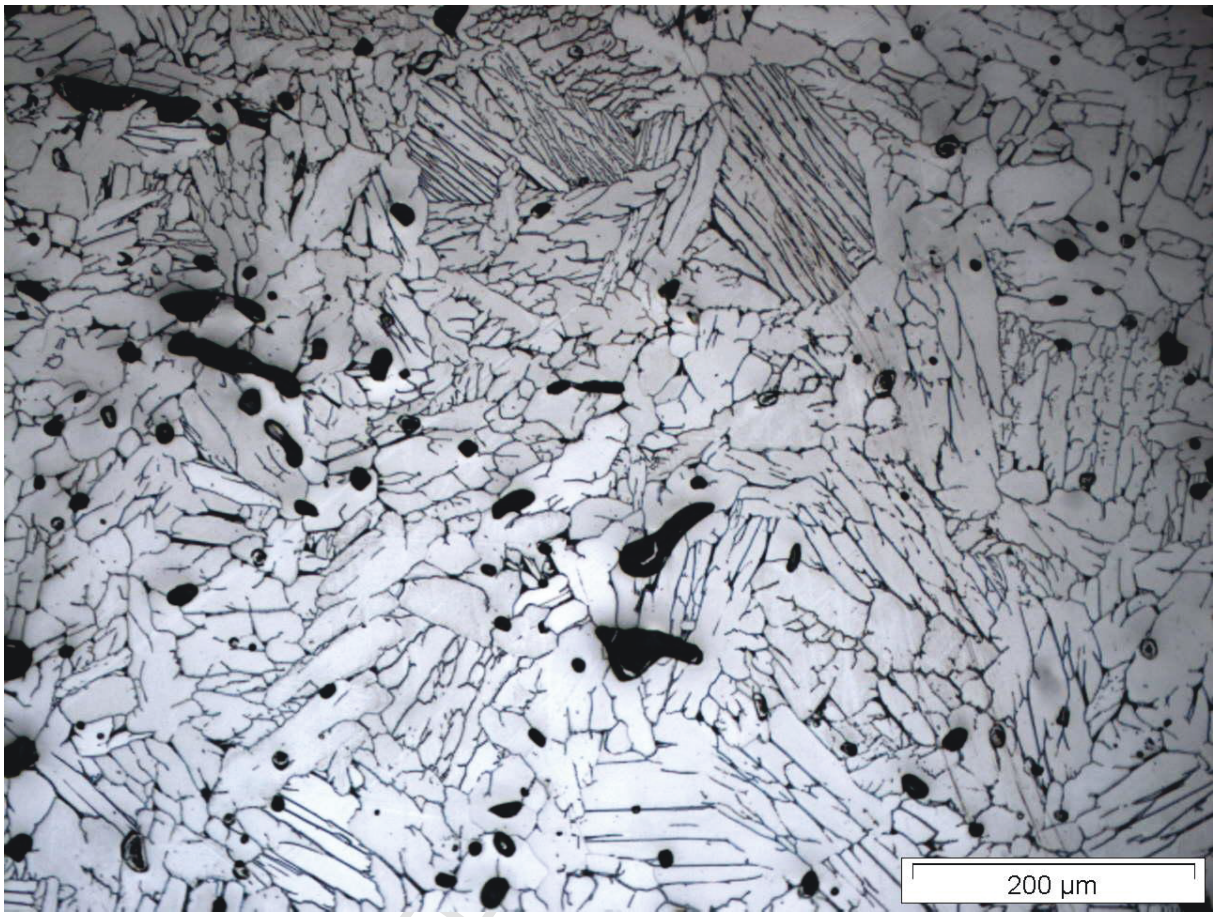

Fig. 3a

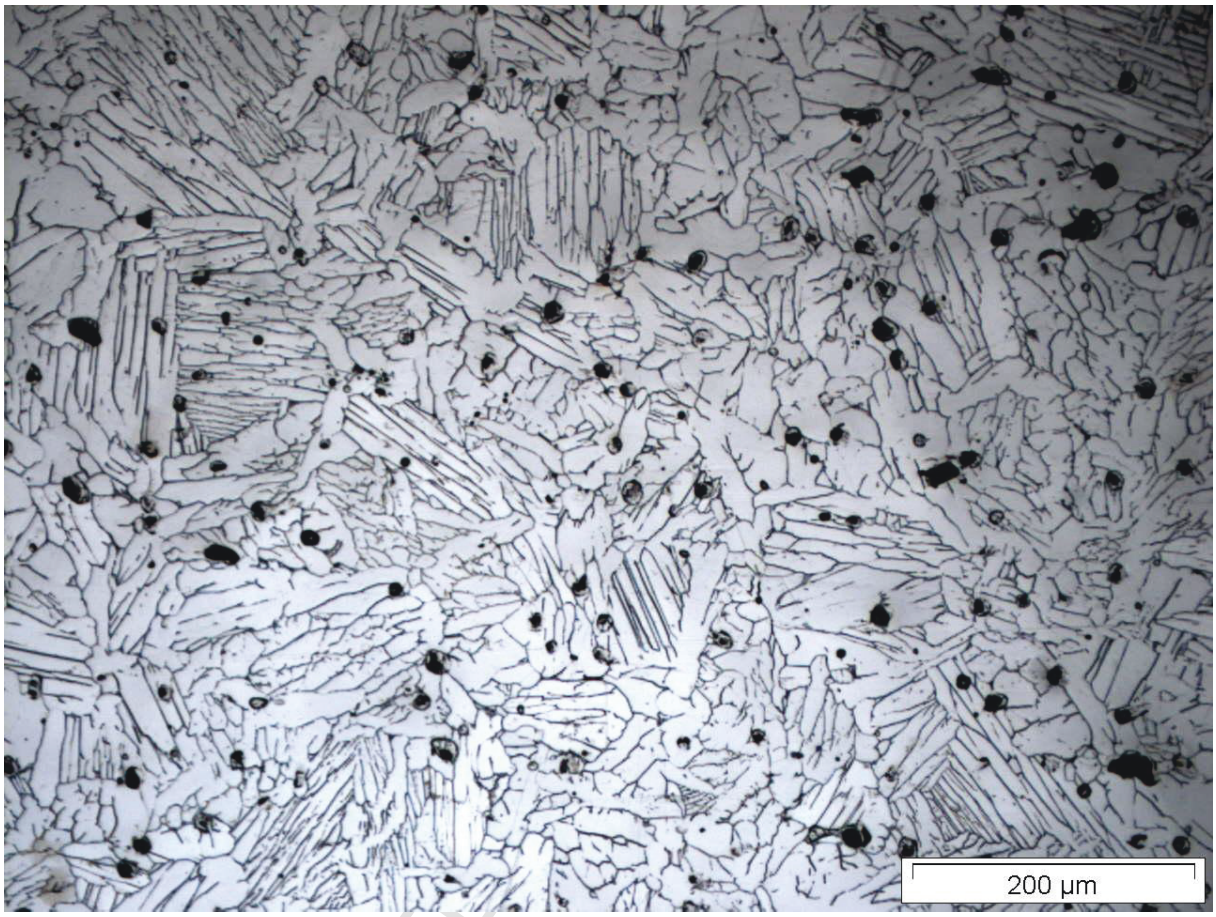

Fig. 3b

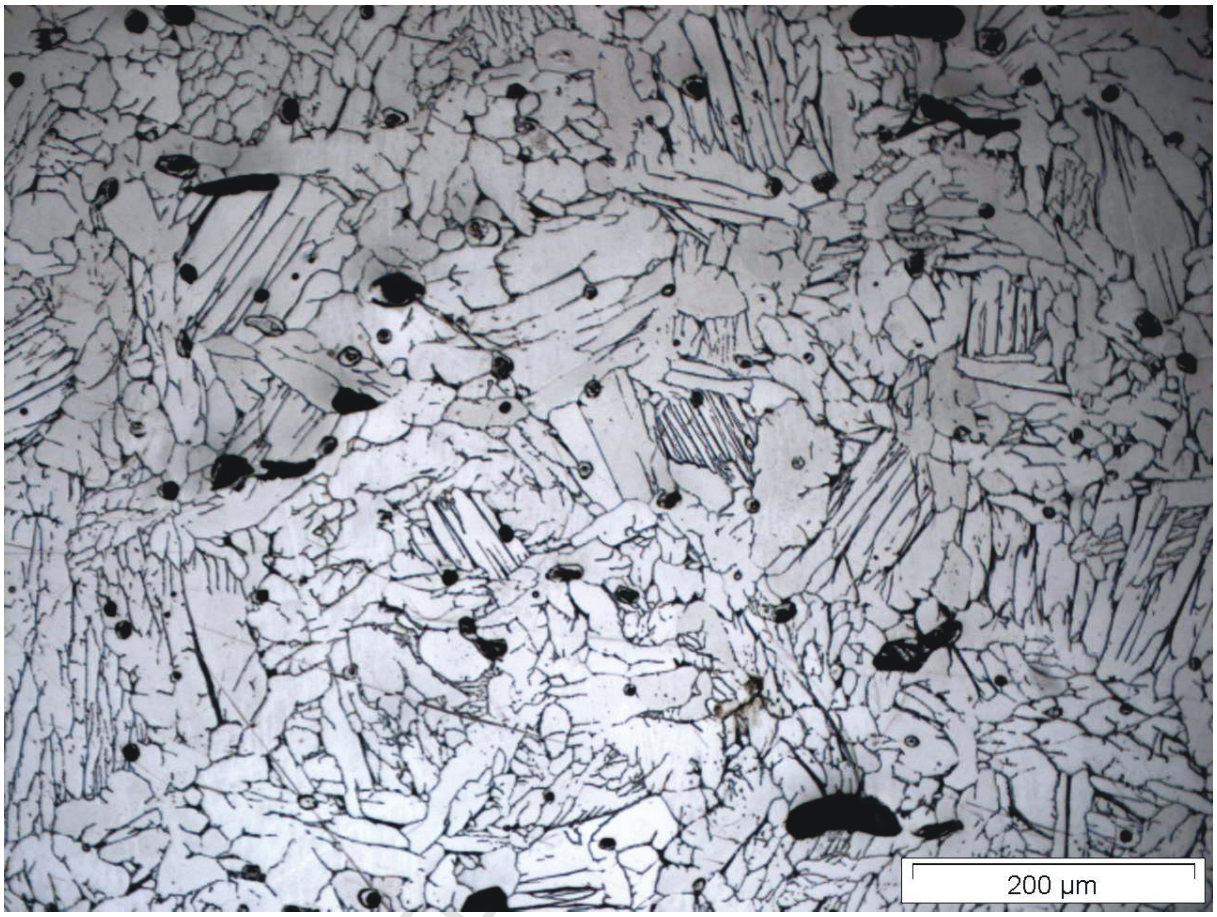

Fig. 3c

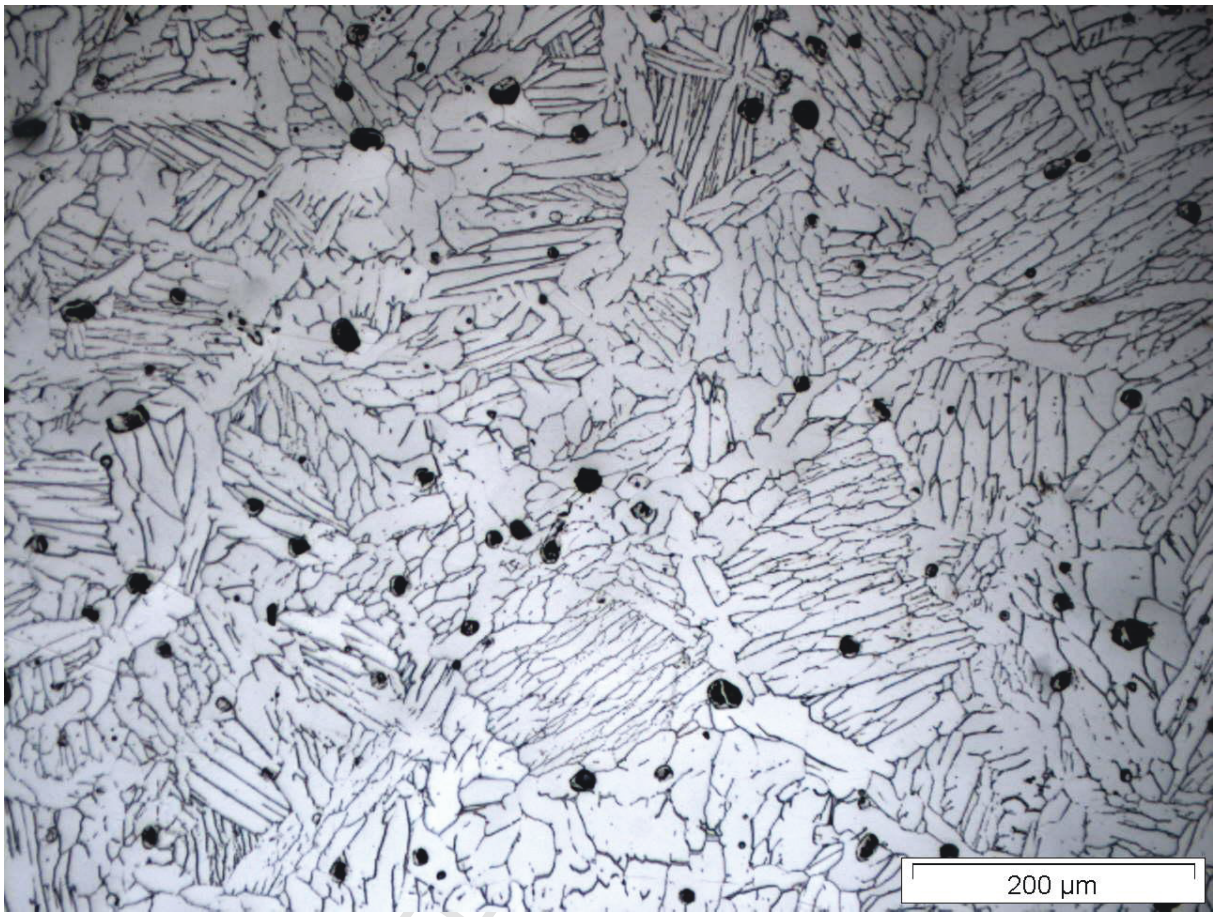

Fig. 3d

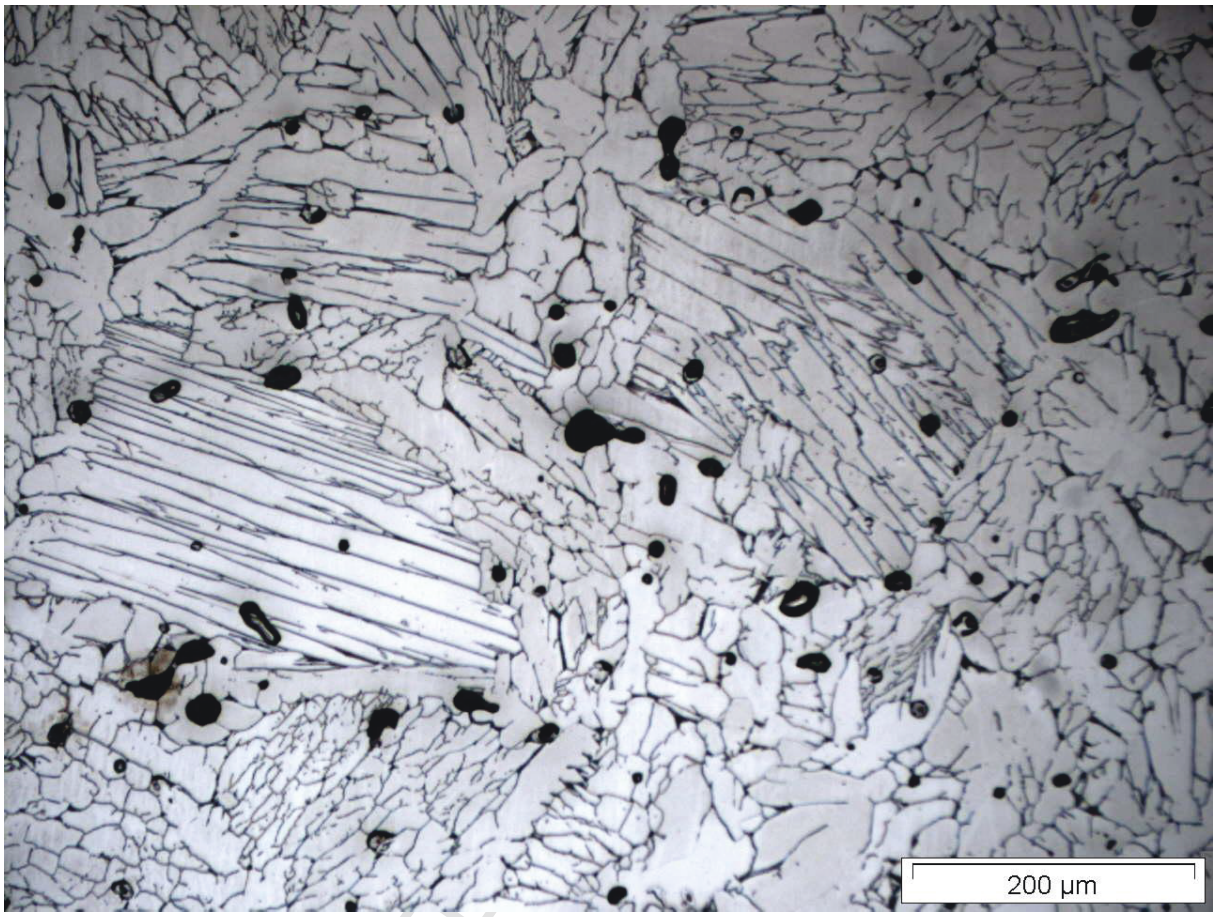

Fig. 3e

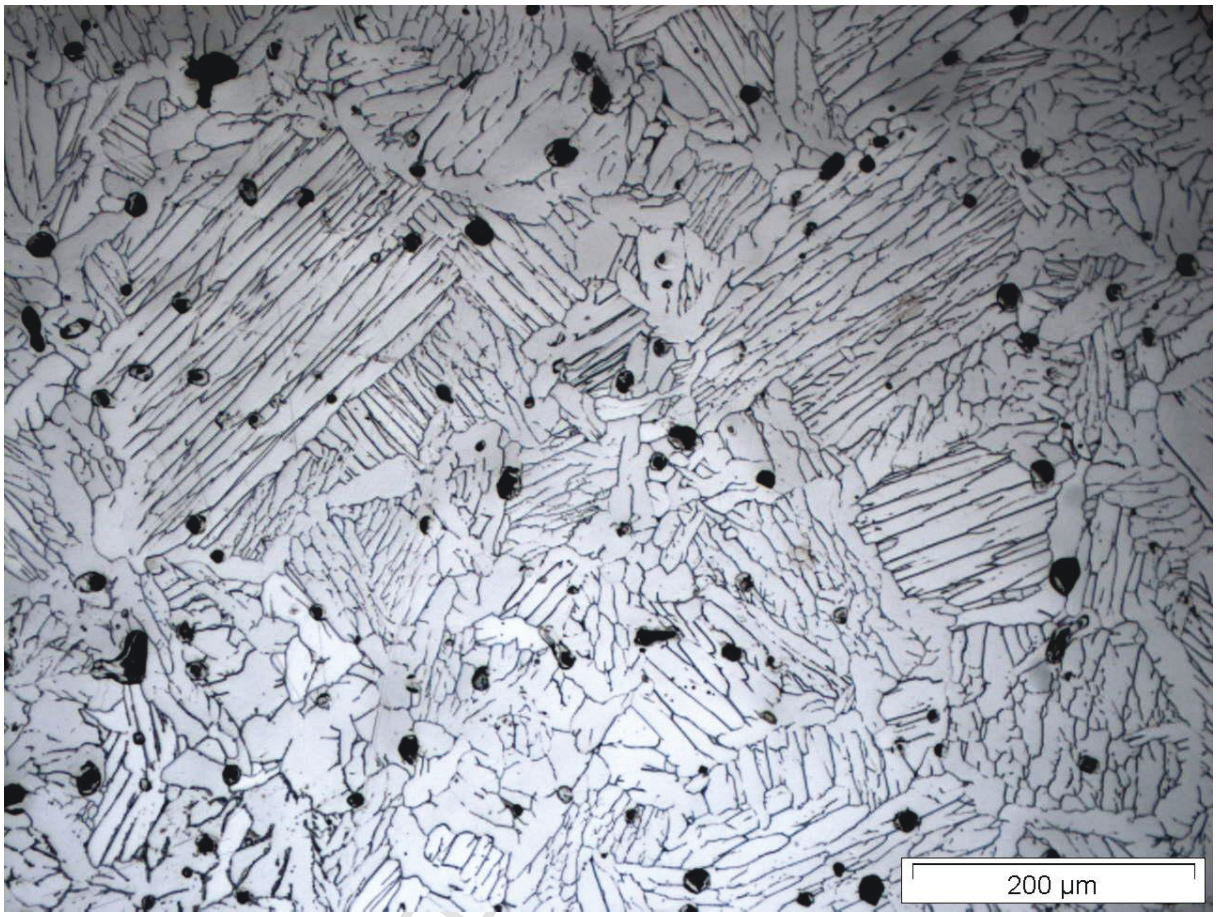

Fig. 3f

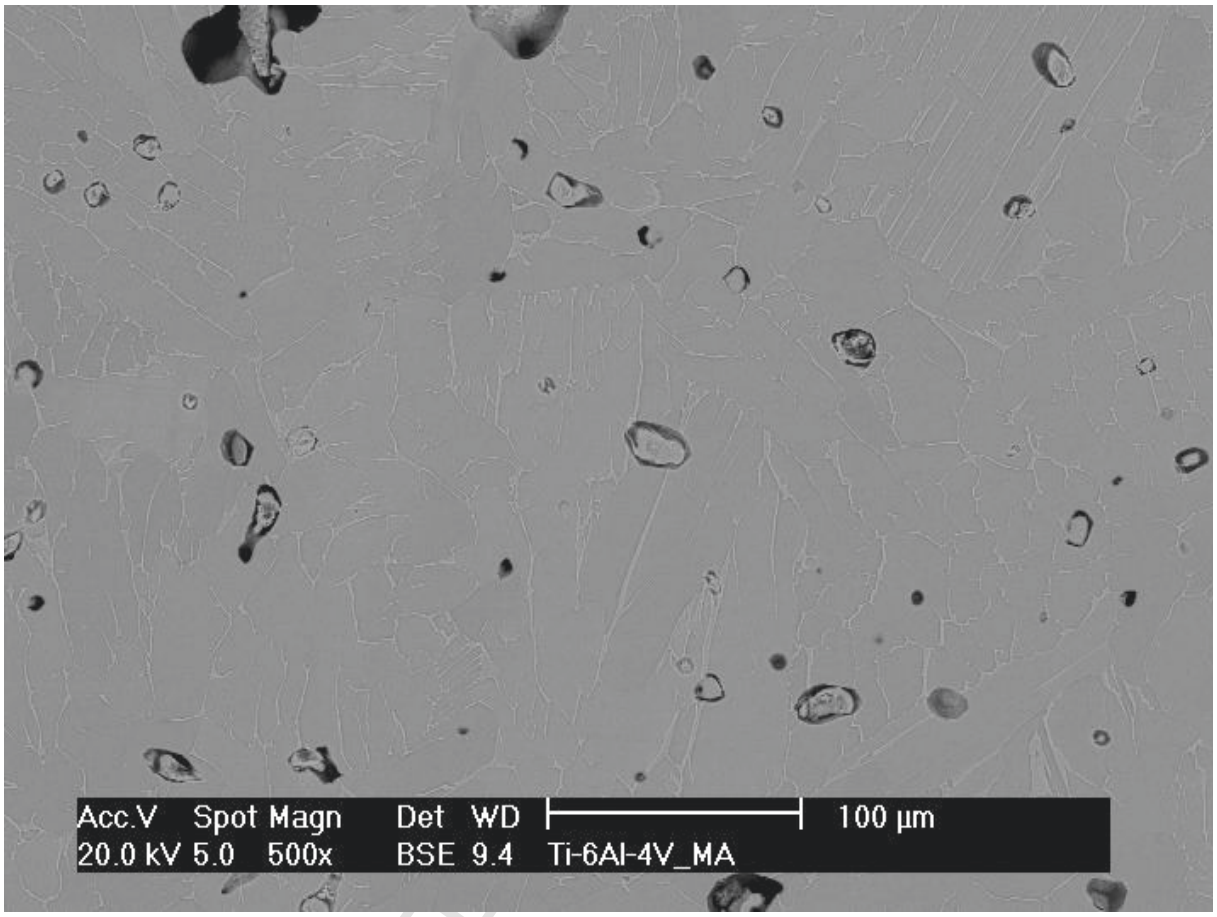

Fig. 4a

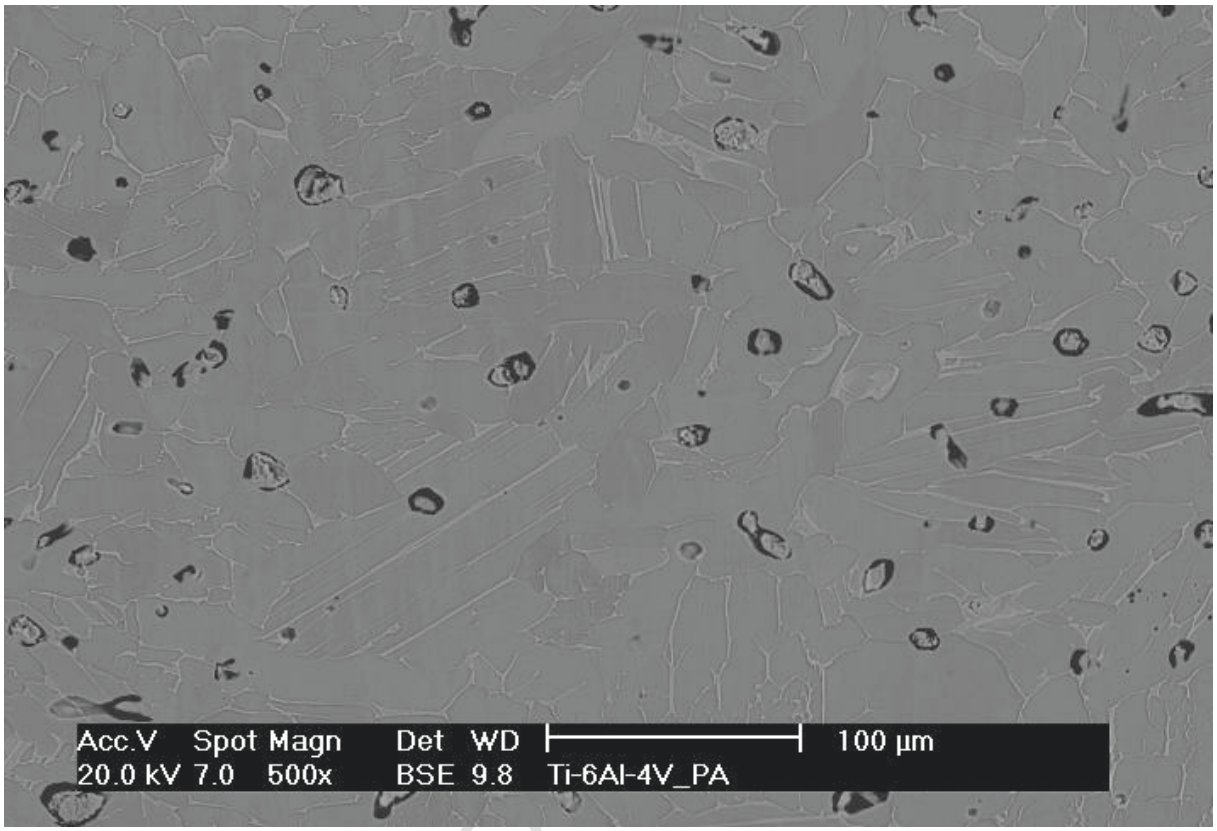

Fig. 4b

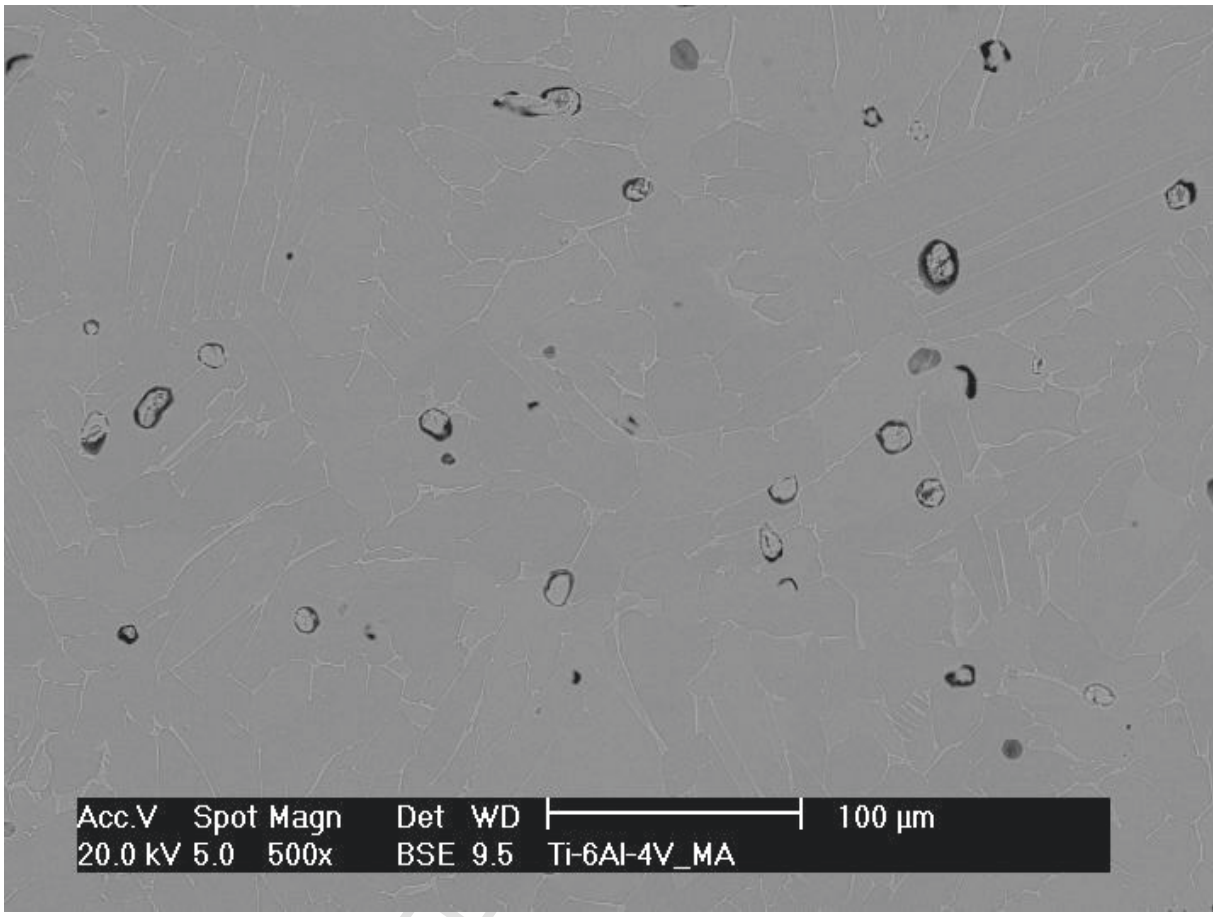

Fig. 4c

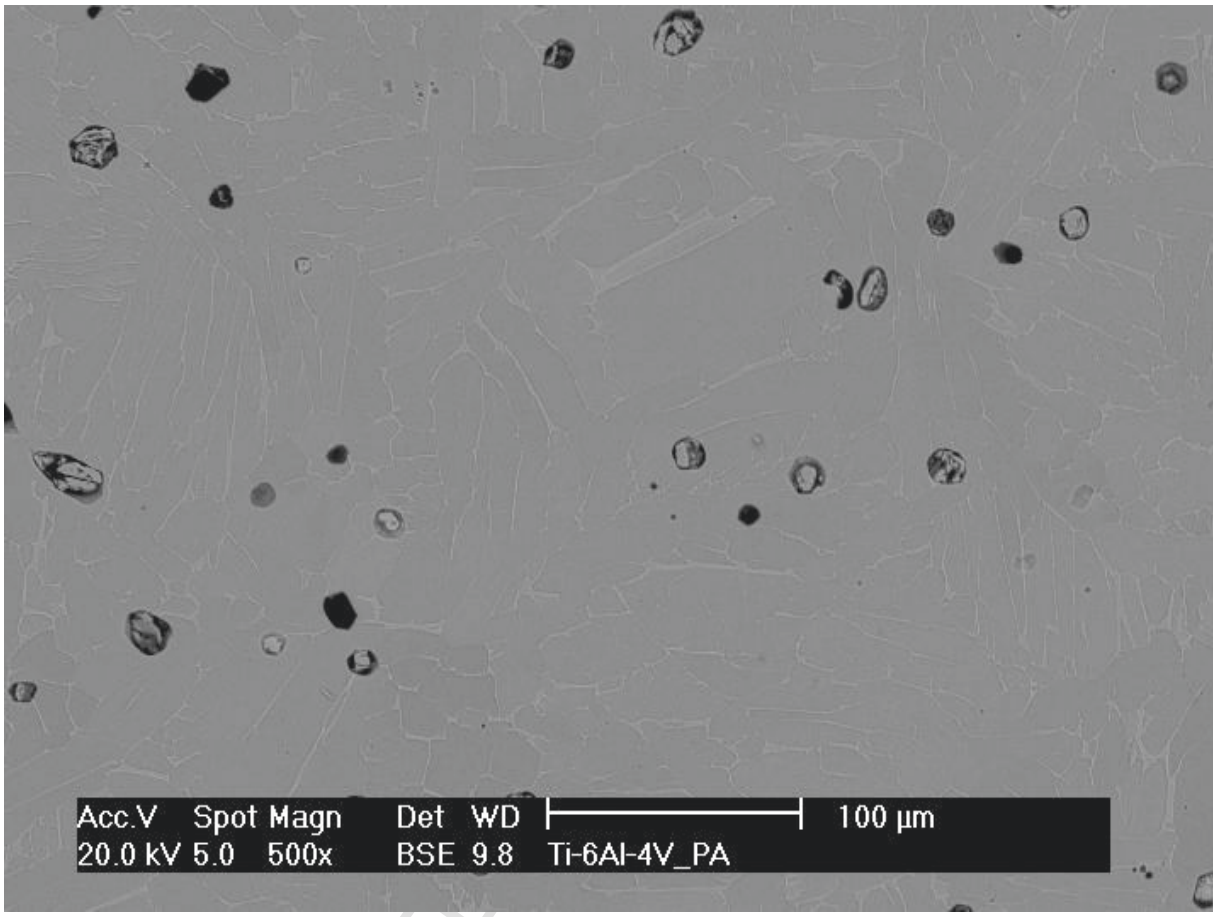

Fig. 4d

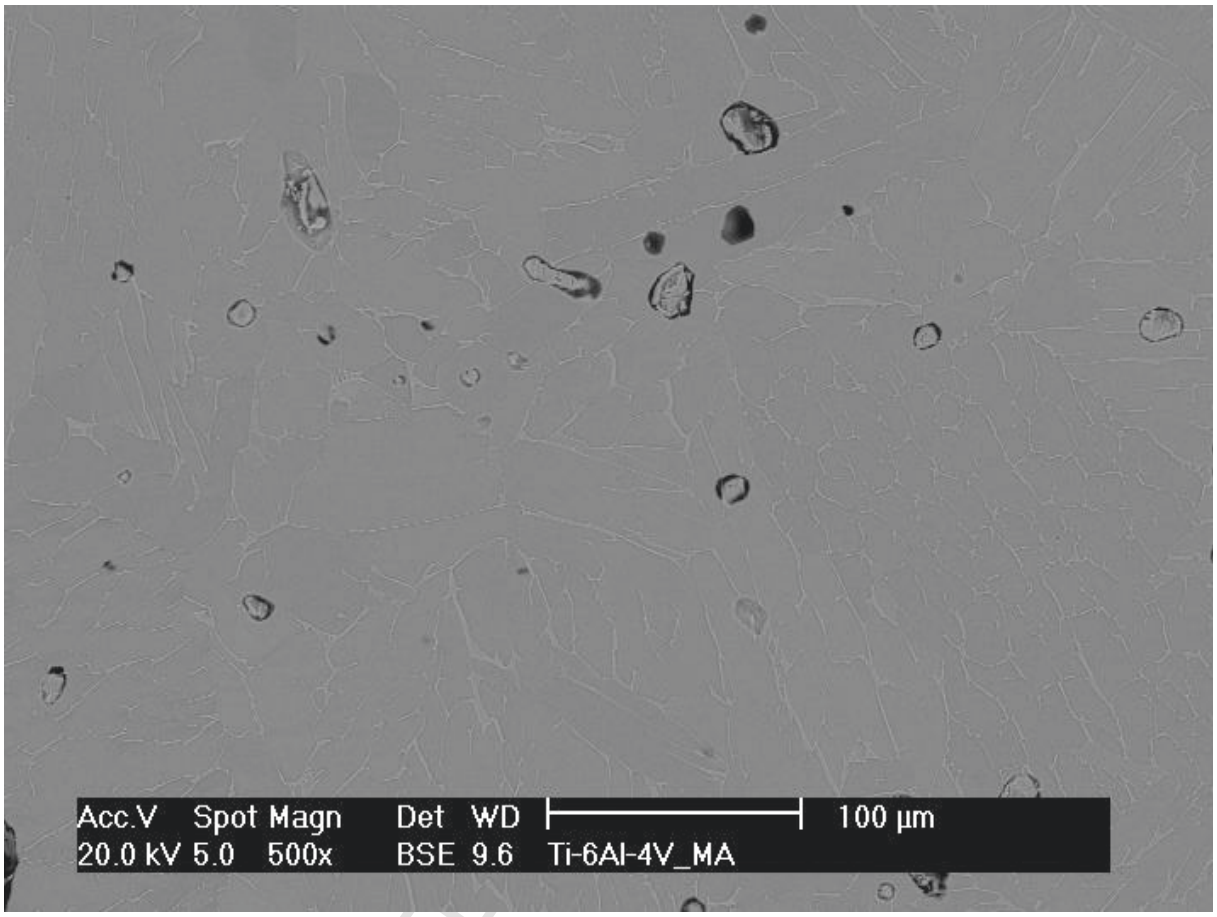

Fig. 4e

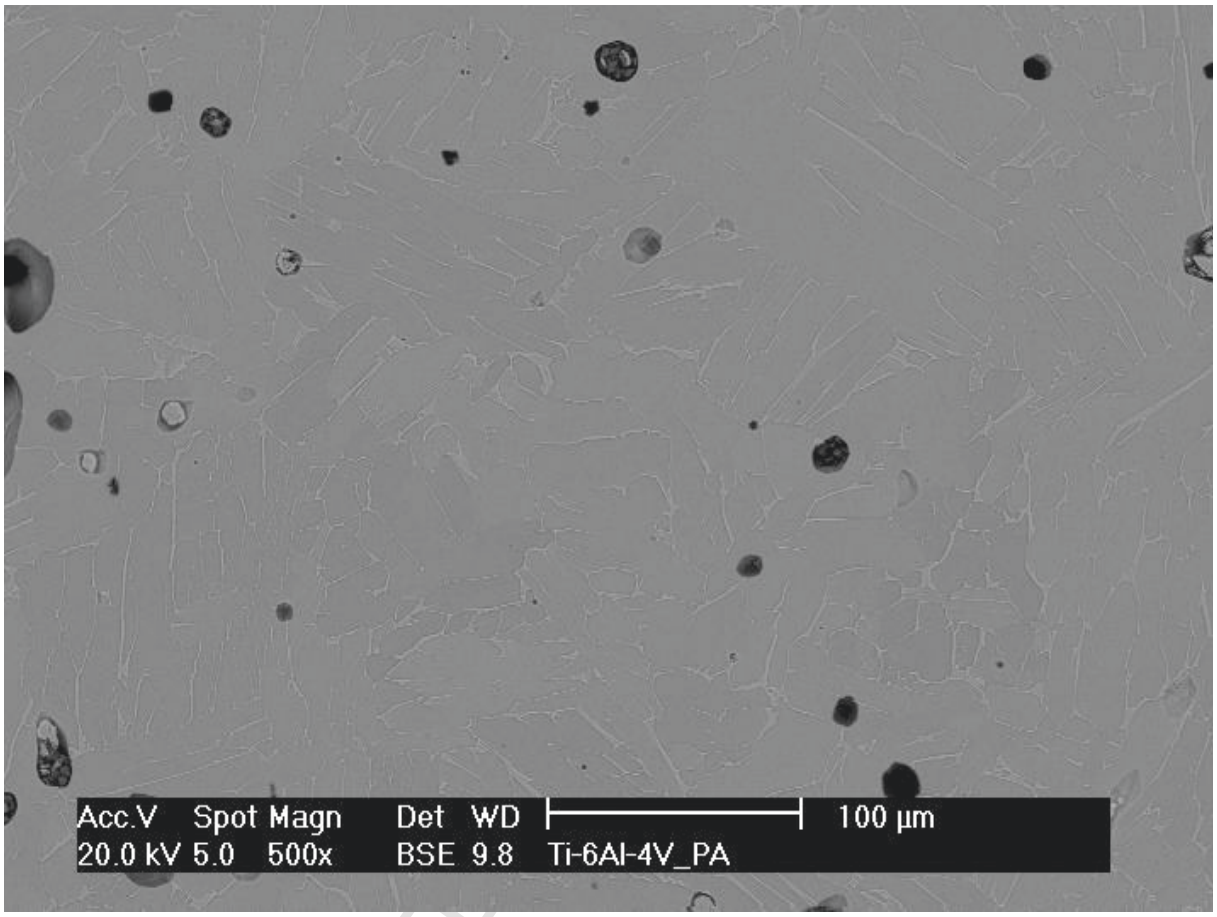

Fig. 4f

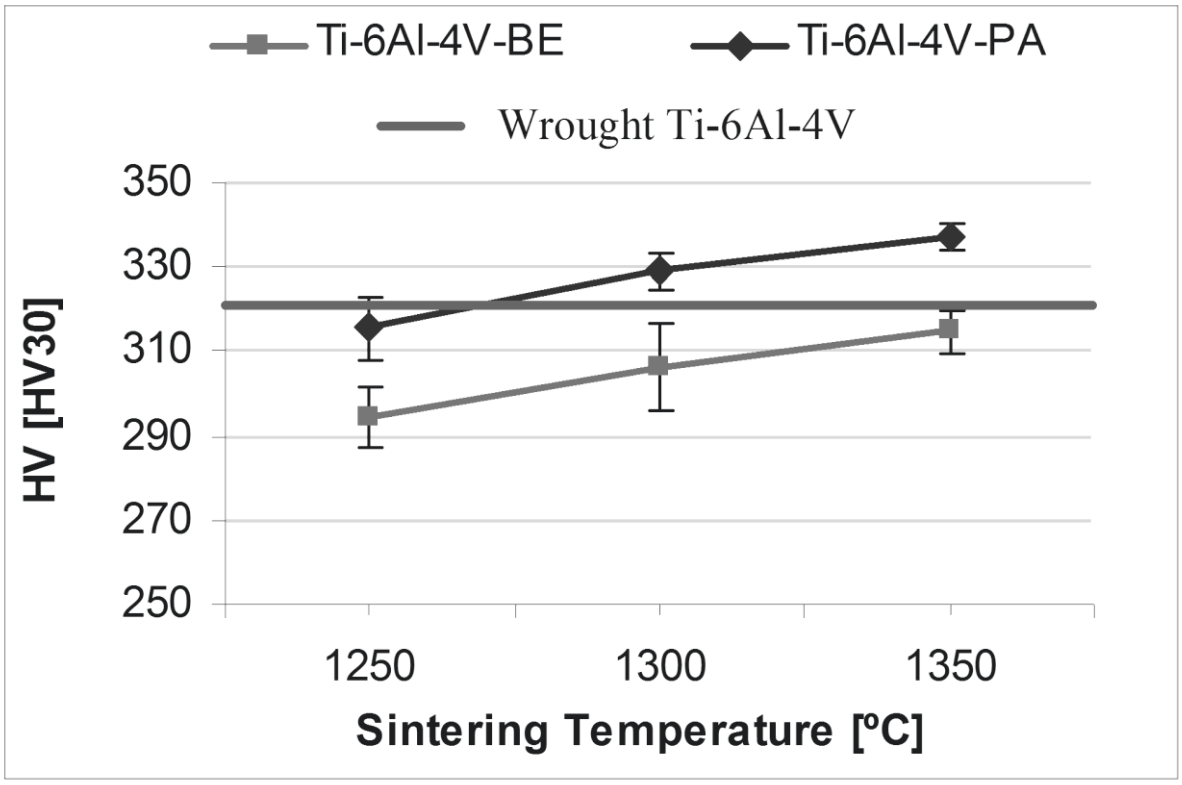

Fig. 5

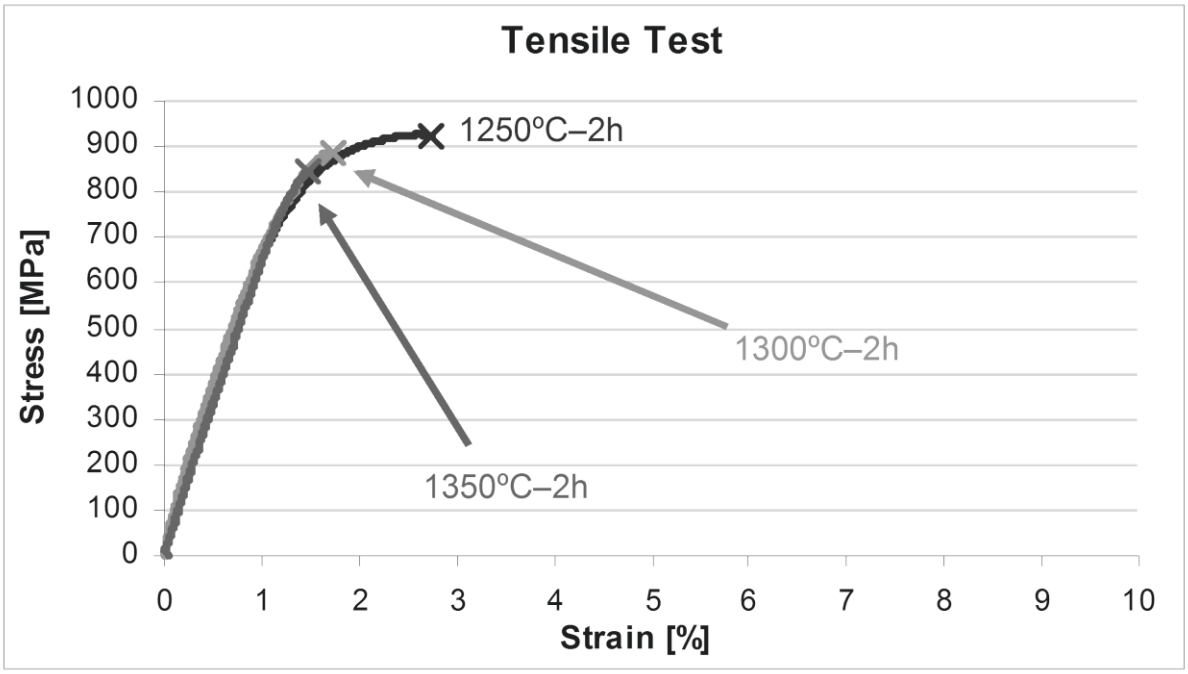

Fig. 6a

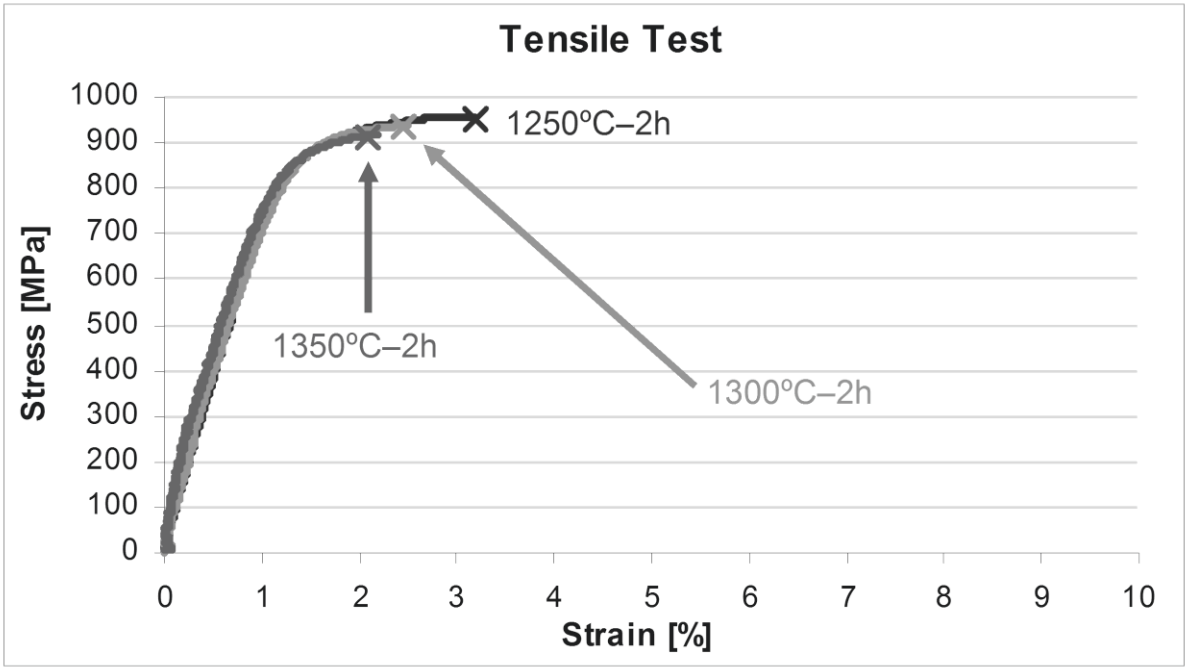

Fig. 6b

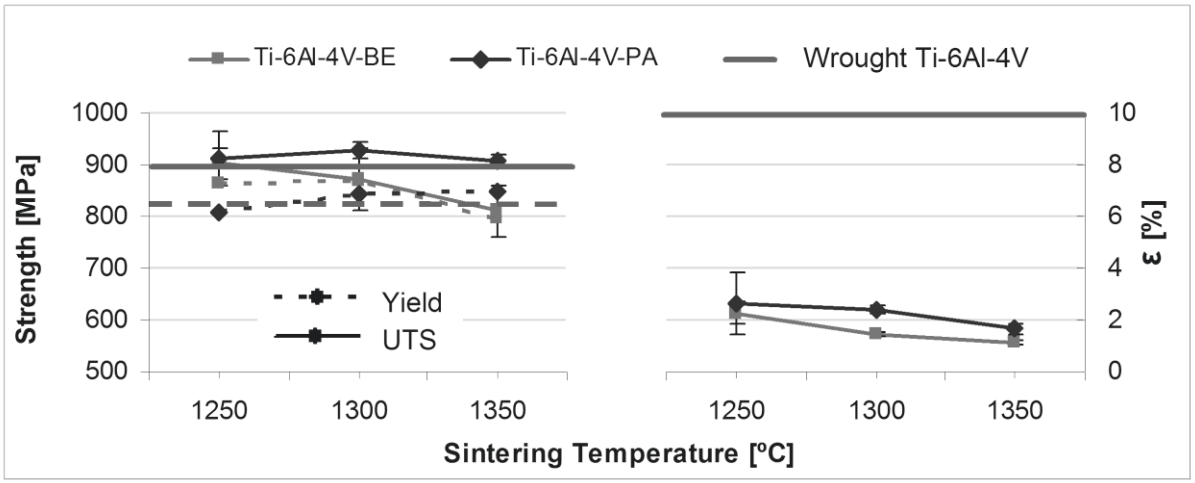

Fig. 7

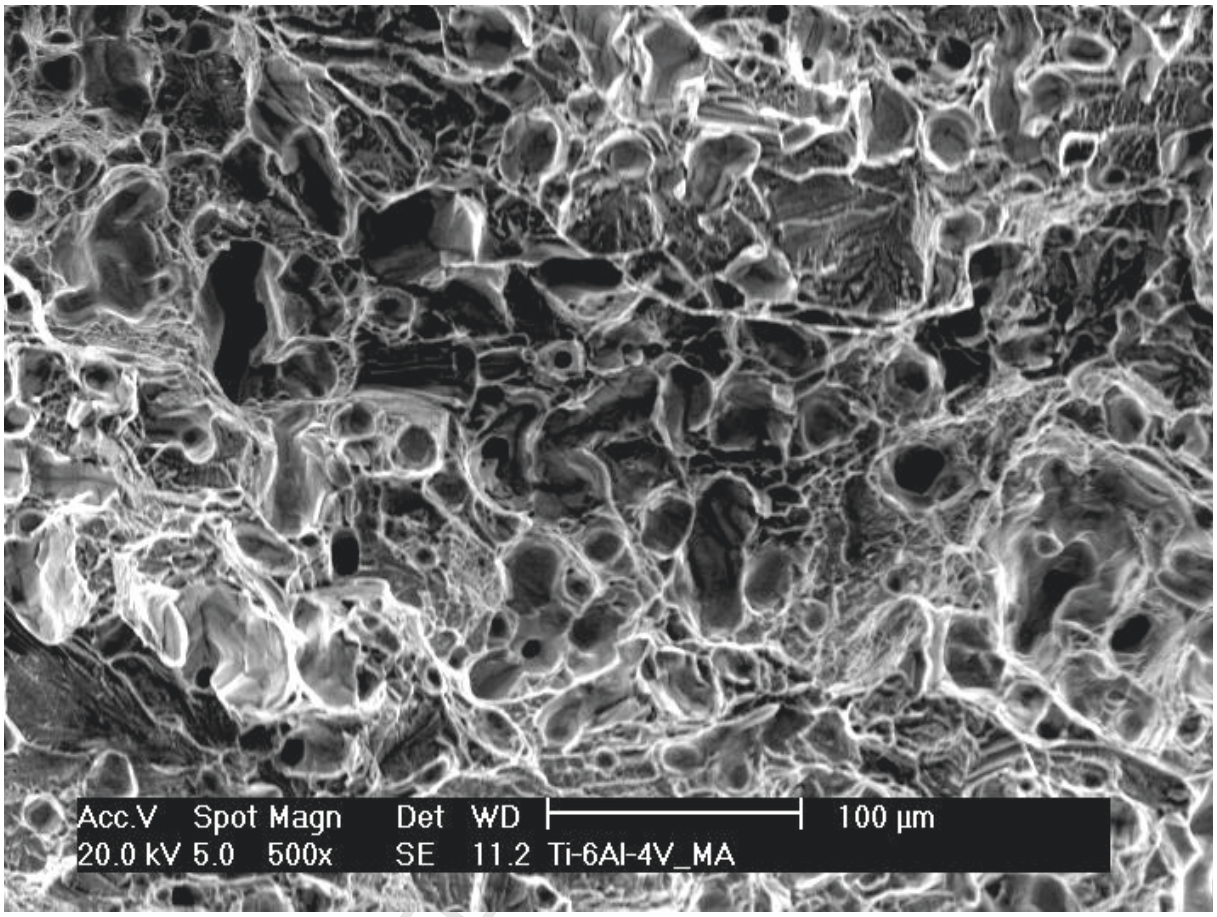

Fig. 8a

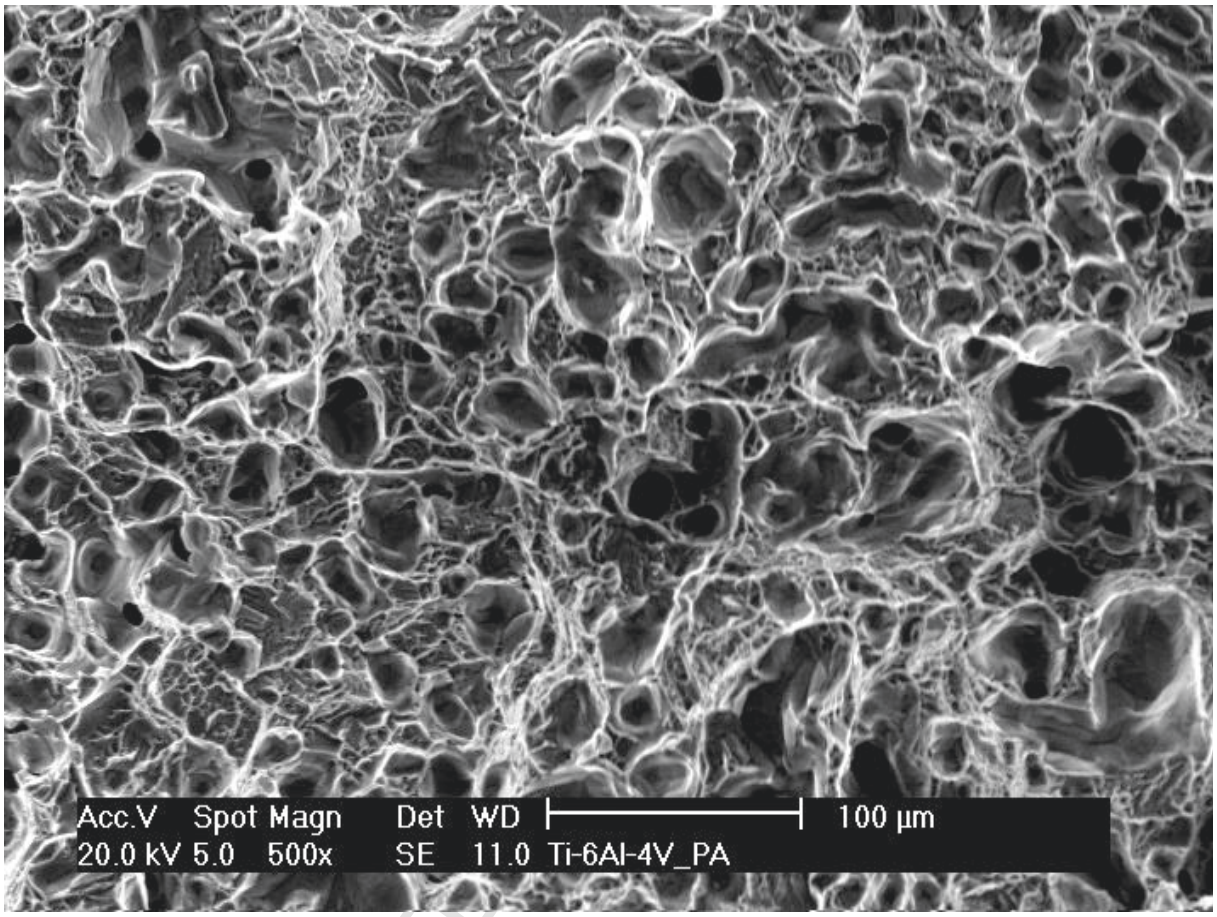

Fig. 8b

Table 1. Oxygen and nitrogen contents of the sintered Ti-6Al-4V-BE and Ti-6Al-4V-PA alloys.

Material	**Processing conditions**	**Interstitials [wt.%]**	
		Oxygen	*Nitrogen*
Ti-6Al-4V-BE	1250ºC-2h	0.44 ± 0.01	0.025 ± 0.006
	1300ºC-2h	0.46 ± 0.05	0.024 ± 0.001
	1350ºC-2h	0.46 ± 0.02	0.023 ± 0.002
Ti-6Al-4V-PA	1250ºC-2h	0.47 ± 0.01	0.023 ± 0.003
	1300ºC-2h	0.51 ± 0.01	0.019 ± 0.006
	1350ºC-2h	0.56 ± 0.03	0.022 ± 0.002

Table 2. EDS chemical composition of the sintered Ti-6Al-4V-BE and Ti-6Al-4V-PA alloys.

Material	**Processing conditions**	*Ti [wt.%]*	*Al [wt.%]*	*V [wt.%]*
Ti-6Al-4V-BE	1250ºC-2h	90.14	5.97	3.89
	1300ºC-2h	90.30	5.89	3.81
	1350ºC-2h	89.64	6.21	4.15
Ti-6Al-4V-PA	1250ºC-2h	90.05	5.81	4.14
	1300ºC-2h	89.91	6.25	3.84
	1350ºC-2h	90.13	6.09	3.78

Table 3. Dynamic Young modulus results of the sintered Ti-6Al-4V-BE and Ti-6Al-4V-PA alloys.

Material	**Processing conditions**	**Young modulus [GPa]**	
Ti-6Al-4V-BE	1250ºC-2h	112 ± 3	*Mean value:* 111 ± 6
	1300ºC-2h	104 ± 1	
	1350ºC-2h	116 ± 1	
Ti-6Al-4V-PA	1250ºC-2h	109 ± 1	*Mean value:* 110 ± 1
	1300ºC-2h	111 ± 2	
	1350ºC-2h	110 ± 1	
Ti-6Al-4V	Wrought	114	

Highlights

> The production of the biomedical Ti-6Al-4V alloy by powder metallurgy is assessed.

> The prealloyed and master alloy addition approaches are considered and compared.

> An in-depth study of the mechanical performances of the materials is carried out.

> The dynamic Young modulus of the alloys developed was determined.